JCTC Journal of Chemical Theory and Computation

Article

pubs.acs.org/JCTC

# Mode Robustness in Raman Optical Activity

Matteo Tommasini,*[,‡,¶] Giovanna Longhi,*[,§,†] Giuseppe Mazzeo,[§,†] Sergio Abbate,[§,†] Belén Nieto-Ortega,[∥] Francisco J. Ramírez,[∥] Juan Casado,[∥] and Juan Teodomiro López Navarrete[∥]

[‡]Dipartimento di Chimica, Materiali e Ingegneria Chimica − Politecnico di Milano, Piazza Leonardo da Vinci, 32 − 20133 Milano, Italy,

[¶]Consorzio Interuniversitario per la Scienza e Tecnologia dei Materiali (INSTM), Unità di Ricerca del Politecnico di Milano (Dip. CMIC), Piazza Leonardo da Vinci 32, 20133 Milano, Italy,

[§]Dipartimento di Medicina Molecolare e Traslazionale − Università di Brescia, Viale Europa 11 − 25123 Brescia, Italy,

[†]C.N.I.S.M. Consorzio Interuniversitario Scienze Fisiche della Materia, c/o Università Roma 3, via della Vasca Navale 84, 00146 Roma, Italy, and

[∥]Department of Physical Chemistry, University of Málaga, 29071 Málaga, Spain

Supporting Information

**ABSTRACT:** By reformulating Raman and ROA invariants we provide ground for the definition of robust modes in ROA spectroscopy. Introduction of two parameters defining robustness helps characterization and assignment of ROA bands. Application and use of robustness parameters to [*n*]helicenes and oxirane/thiirane derivatives are presented.

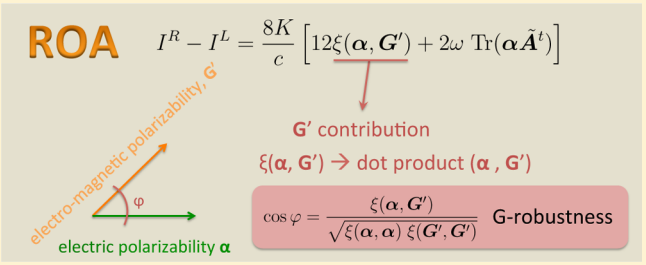


## 1. INTRODUCTION

The analysis and assignment of Raman Optical Activity (ROA) vibrational spectra[1−4] has been greatly helped by the availability of reliable quantum chemical tools[5−12] for the calculation of the molecular tensors involved in this chiroptical variant of Raman spectroscopy. The relevant quantities are the vibrational transition moments of quantities defined respectively by the real part of the products of the electric dipole-electric dipole (polarizability tensor) $\boldsymbol{\alpha}$, by the imaginary part of the electric dipole-magnetic dipole tensor $\boldsymbol{G}'$, and by the real part of the traceless electric dipole-electric quadrupole tensor $\boldsymbol{A}$.[1,3] Most theoretical analysis of ROA spectra is conducted in the far from resonance (FFR) frame, to which we comply in the present work.

When employing theoretically derived ROA intensity data to assign observed peaks and to relate them to molecular structure information, it is desirable to associate the above molecular tensors as transparently as possible to the physically measured quantities. This can be conveniently done by unveiling the algebraic structure which is associated with the celebrated expressions of ROA intensity[13] (see also the review by Barron and Buckingham[14]). As it will be shown in this work, this kind of analysis naturally allows to extend to ROA spectroscopy the concept of *robust modes* which was initially introduced in Vibrational Circular Dichroism (VCD) by Nicu et al.[15] and discussed later.[16,17]

The robustness concept for the ROA bands that we are about to introduce will be defined for the SCP backscattering geometry.[1−4] The latter one is the most commonly employed geometry of scattering in commercial instruments.[3,4] Besides, in the FFR frame SCP and ICP expression for intensities are the same[3,4] and also the same as $DCP_I$; thus the results derived here may be translated to several scattering geometries.

## 2. THEORY

Based on Barron and Buckingham work, the ROA intensity of a given vibrational normal mode of a molecule in solution state can be expressed in terms of the anisotropy ($\beta$) of the molecular tensors introduced above:

$$I^R - I^L = \frac{8K}{c}[12\beta(\boldsymbol{G}')^2 + 4\beta(\boldsymbol{A})^2] \tag{1}$$

The corresponding Raman intensity is given by

$$I^R + I^L = 4K[5\mathrm{Tr}(\boldsymbol{\alpha})^2 + 7\beta(\boldsymbol{\alpha})^2] \tag{2}$$

where $c$ is the speed of light, $K$ is a constant [For the exact definition of $K$, see for example refs 3 and 4.], and Tr represents the trace. The $\beta$-terms are explicitly defined as follows:

$$\beta(\boldsymbol{\alpha})^2 = \frac{1}{2}\sum_{ij}(3\alpha_{ij}\alpha_{ij} - \alpha_{ii}\alpha_{jj});$$
$$\beta(\boldsymbol{G}')^2 = \frac{1}{2}\sum_{ij}(3\alpha_{ij}G'_{ij} - \alpha_{ii}G'_{jj});$$
$$\beta(\boldsymbol{A})^2 = \frac{1}{2}\omega\sum_{ijkl}\alpha_{ij}\varepsilon_{ikl}A_{k,lj} \tag{3}$$

**Received:** August 1, 2014
**Published:** November 13, 2014

   dx.doi.org/10.1021/ct500697e | J. Chem. Theory Comput. 2014, 10, 5520−5527

In the expression of $\beta(\boldsymbol{A})^2$ the $\varepsilon_{ijk}$ term is the Levi-Civita symbol, which in three dimensions can be expressed as $\varepsilon_{ijk} = (i - j)(j - k)(k - i)/2$, provided that the Cartesian indices $i, j, k$ assume values in the set (1,2,3).

It is instructive to analyze the behavior of $\beta$-terms upon a linear transformation of the tensors involved in their definition. For instance, according to eq 3, one easily finds that $\beta(\lambda\boldsymbol{\alpha})^2 = \lambda^2\beta(\boldsymbol{\alpha})^2$ (for an arbitrary real $\lambda$). Furthermore, (see the Supporting Information) $\beta(\boldsymbol{a} + \boldsymbol{b})^2$ behaves as follows:

$$\beta(\boldsymbol{a} + \boldsymbol{b})^2 = \beta(\boldsymbol{a})^2 + \beta(\boldsymbol{b})^2 + 2\xi(\boldsymbol{a}, \boldsymbol{b}) \tag{4}$$

where $\xi$ has been introduced to provide common ground for one- and two-matrix properties of eqs 3. It is defined as

$$\xi(\boldsymbol{a}, \boldsymbol{b}) = \frac{1}{2}\sum_{ij}[3a_{ij}b_{ij} - a_{ii}b_{jj}] \tag{5}$$

We note that, by the definition (5) and by eq 3, it is $\xi(\boldsymbol{a}, \boldsymbol{a}) = \beta(\boldsymbol{a})^2$. As anticipated above, this allows to directly write $\beta$-terms showing in the expression of Raman and ROA intensities through $\xi$:

$$\begin{aligned}\beta(\boldsymbol{\alpha})^2 &= \xi(\boldsymbol{\alpha}, \boldsymbol{\alpha})\\ \beta(\boldsymbol{G}')^2 &= \xi(\boldsymbol{\alpha}, \boldsymbol{G}')\end{aligned} \tag{6}$$

The use of $\xi$ makes the definition of the $\beta(\boldsymbol{G}')^2$ term more perspicuous by explicitly evidencing the role of *both* $\boldsymbol{G}'$ *and* $\boldsymbol{\alpha}$ tensors. $\xi$ has appealing properties, somewhat concealed by the traditional definition of $\beta$. Right from its definition, eq 5, it is straightforward to show that $\xi$ is positive-definite, linear, commutative, and associative. Hence $\xi(\boldsymbol{a}, \boldsymbol{b})$ behaves as a form of inner product between $\boldsymbol{a}$ and $\boldsymbol{b}$ – where $\boldsymbol{a}$ and $\boldsymbol{b}$ are second order molecular tensors, like $\boldsymbol{\alpha}$ and $\boldsymbol{G}'$ (see Supporting Information, part 1).

Also the $\beta(\boldsymbol{A})^2$ term can be written as inner product. To this aim we carry out the four index sum in two steps, as follows:

$$\beta(\boldsymbol{A})^2 = \frac{1}{2}\omega\sum_{ijkl}\alpha_{ij}\varepsilon_{ikl}A_{k,lj} = \frac{1}{2}\omega\sum_{ij}\alpha_{ij}\sum_{kl}\varepsilon_{ikl}A_{k,lj} \tag{7}$$

The sum over $k,l$ indexes provides us with a second-order tensor which we call $\tilde{\boldsymbol{A}}$:

$$\tilde{A}_{ij} = \sum_{kl}\varepsilon_{ikl}A_{k,lj} \tag{8}$$

Thus, the $\beta(\boldsymbol{A})^2$ term can be written as follows:

$$\beta(\boldsymbol{A})^2 = \frac{1}{2}\omega\sum_{ij}\alpha_{ij}\tilde{A}_{ij} = \frac{1}{2}\omega\mathrm{Tr}[\boldsymbol{\alpha}\tilde{\boldsymbol{A}}^t] \tag{9}$$

($\tilde{\boldsymbol{A}}^t$ indicates the transpose of $\tilde{\boldsymbol{A}}$). Equation 9 sets $\beta(\boldsymbol{A})^2$ as the Frobenius product of the matrices (tensors) $\boldsymbol{\alpha}$ and $\tilde{\boldsymbol{A}}$. The Frobenius product is well-known to behave as an inner product between matrices. We notice here the difference between the $\xi$-inner product and the Frobenius one, the former being defined as a Frobenius product minus the product of the traces of the two tensors (i.e., the isotropic component). We conclude that Raman and ROA intensities can be cast in a form where (apart from the simple case of $\mathrm{Tr}(\boldsymbol{\alpha})$ in Raman) all required molecular tensor invariants can be expressed as inner products (either $\xi$- or Frobenius-kind):

$$\begin{aligned}I^R + I^L &= 4K[5\mathrm{Tr}(\boldsymbol{\alpha})^2 + 7\xi(\boldsymbol{\alpha}, \boldsymbol{\alpha})]\\ I^R - I^L &= \frac{8K}{c}[12\xi(\boldsymbol{\alpha}, \boldsymbol{G}') + 2\omega\mathrm{Tr}(\boldsymbol{\alpha}\tilde{\boldsymbol{A}}^t)]\end{aligned} \tag{10}$$

The $\xi$-inner product possesses several interesting properties, which directly stem for its definition, eq 5. Details are given in Supporting Information, part 1.

Based on eq 10, where all quantities have been cast in inner product form, we can now propose a straightforward definition of mode robustness in ROA. We define the angle $\varphi$ as the one formed between $\boldsymbol{\alpha}$ and $\boldsymbol{G}'$ tensors with respect to $\xi$-inner product. It is directly related to Barron's $\beta(\boldsymbol{G}')^2$ term in the expression of ROA, and its cosine is naturally given by the $\xi$-inner product of $\boldsymbol{\alpha}$ and $\boldsymbol{G}'$, divided by the square root of the $\xi$-norm of $\boldsymbol{\alpha}$ and $\boldsymbol{G}'$, i.e.:

$$\cos\varphi = \frac{\xi(\boldsymbol{\alpha}, \boldsymbol{G}')}{\sqrt{\xi(\boldsymbol{\alpha}, \boldsymbol{\alpha})\xi(\boldsymbol{G}', \boldsymbol{G}')}} \tag{11}$$

Similarly, the angle $\psi$ is associated with Barron's $\beta(\boldsymbol{A})^2$ term and originates directly from the Frobenius inner product between $\boldsymbol{A}$ and $\boldsymbol{\alpha}$ tensors:

$$\cos\psi = \frac{\mathrm{Tr}(\boldsymbol{\alpha}\tilde{\boldsymbol{A}}^t)}{\sqrt{\mathrm{Tr}(\boldsymbol{\alpha}\boldsymbol{\alpha}^t)\mathrm{Tr}(\tilde{\boldsymbol{A}}\tilde{\boldsymbol{A}}^t)}} \tag{12}$$

Equations 11 and 12 may be used to introduce the concept of robustness in ROA. Accordingly, we may introduce the terms G-robustness and A-robustness when the related molecular tensors are implied; alternatively, when the associated angles are under discussion, we may respectively speak about $\varphi$-robustness and $\psi$-robustness.

## 3. APPLICATION TO HELICENES

It has been recently shown that ROA spectroscopy carries interesting information on the molecular structure of helicenes (2-Br-hexahelicene being a representative example[18]). Hence, we apply here to the [$n$]helicenes series ($n$ = 4–16) the theoretical analysis of the ROA tensors introduced above, and we examine the mode robustness of the strongest ROA signal of these systems, which corresponds to the D peak of molecular graphenes.[18,19] To ease the computational burden and to allow the exploration of a wider range in molecular size, we limit ourselves to DFT calculations at the B3LYP/6-31G(d,p) level. Gaussian09 has been used to carry out all calculations,[20] and a custom code has been written on purpose to carry out the analysis of ROA tensors starting from Gaussian formatted checkpoint files. In Figure 1 we report the simulated Raman and ROA spectra ($\lambda_{exc}$ = 532 nm) of the series of [$n$]helicenes for increasing molecular size. Two conclusions can be drawn from inspecting the plots: (i) as $n$ increases, the D signal becomes progressively stronger with respect to other weaker spectral features both in Raman and ROA; (ii) the D peak red-shifts as $\pi$-conjugation increases with $n$. Both facts are known in Raman spectroscopy of achiral $\pi$-conjugated compounds (with either linear conjugation or planar conjugation, as in graphenes[19]). Indeed, the extension of these results to ROA spectroscopy of chiral $\pi$-conjugated compounds may be expected. In Figure 2 we show that ROA tensor analysis and robustness provide a clear insight into the reasons for the selectivity and strength of the D signal in ROA. The plot in Figure 2 displays the values of the robustness angles $\varphi$, $\psi$ vs the dipolar and quadrupolar contributions to ROA intensities, i.e., $\xi(\boldsymbol{\alpha}, \boldsymbol{G}')$ and $\mathrm{Tr}(\boldsymbol{\alpha}\tilde{\boldsymbol{A}}^t)$, respectively. Red points show the dipolar component of ROA and $\varphi$ angles; blue points show the quadrupolar contributions and $\psi$ angles. Each data point in Figure 2 comes from a normal mode in the D peak region whose ROA intensity falls within 90%


dx.doi.org/10.1021/ct500697e | J. Chem. Theory Comput. 2014, 10, 5520–5527

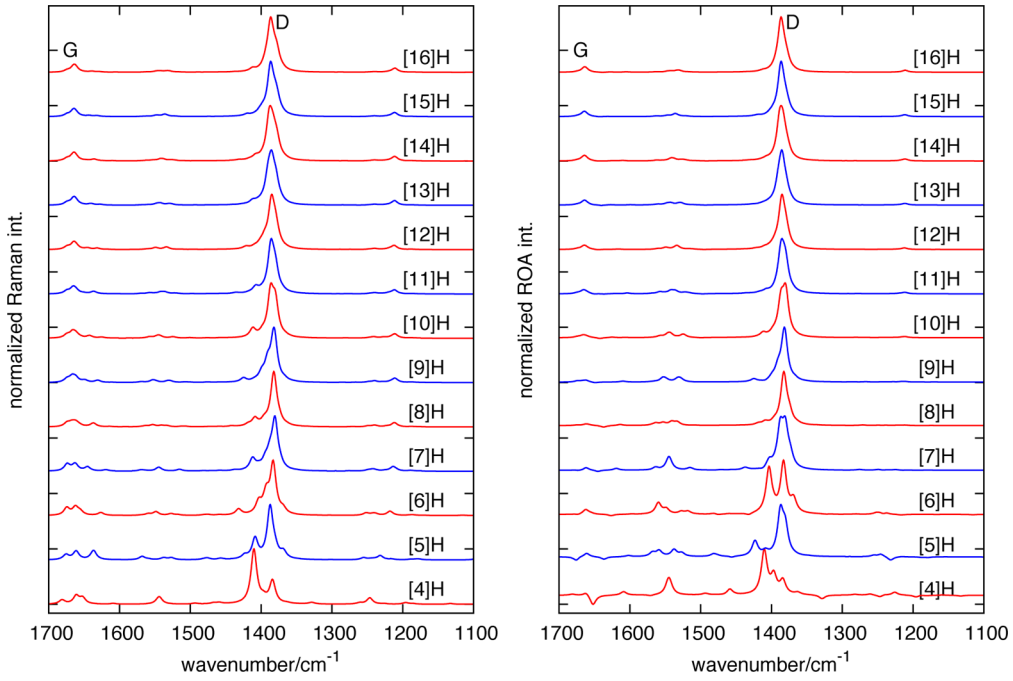


**Figure 1.** Simulated Raman (left panel) and ROA (right panel) spectra of [*n*]helicenes of increasing size (*n* = 4−16) in the region of the G and D peaks.[18] Intensity and wavenumber data have been obtained from DFT calculations carried out at the B3LYP/6-31G(d,p) level. Spectra have been simulated by summing Lorentzian line shapes whose areas are proportional to the computed Raman (ROA) intensity, centered at computed vibrational frequencies. The fwhm of the Lorentzian line shapes was fixed at 10 $cm^{-1}$, and all spectra have been normalized to the strongest calculated peak.

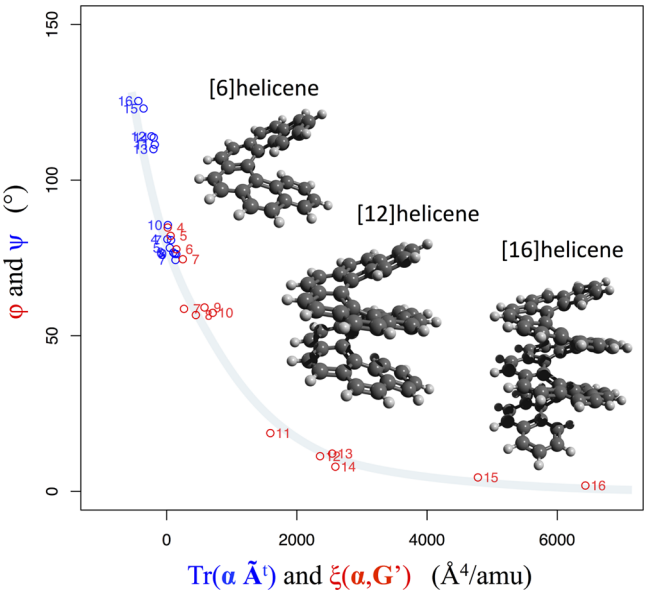


**Figure 2.** Robustness angles $\varphi$ and $\psi$ as a function of the magnetic dipolar and electric quadrupolar contributions to ROA intensity (see eq 10). Red points denote dipolar pairs ($\xi(\boldsymbol{\alpha}, \boldsymbol{G}')$, $\varphi$); blue points denote quadrupolar pairs ($\mathrm{Tr}(\boldsymbol{\alpha}\tilde{\boldsymbol{A}}^t)$, $\psi$). As a reference for a better reading of the clustered points in the plot the interested reader may refer to the Supporting Information (Table SI.1).

of the maximum ROA intensity of a given [*n*]helicene. To facilitate reading of the data, the number *n* of fused benzene rings giving rise to helicenes is also reported for each data point. The data clearly reveal that, as *n* increases, the dipolar contribution to ROA largely exceeds the quadrupolar contribution. Furthermore, in larger helicenes the D peak progressively becomes more robust, as proved by the value of the $\varphi$ angle which approaches zero. On the other hand, the $\psi$ angle is far from robust values in smaller helicenes, inverts its sign, and heads to −180° in longer helicenes. This shows that with increasing *n*, the $\boldsymbol{G}'$ and $\boldsymbol{\alpha}$ tensors of the D peak progressively become "more parallel" (since helicity builds up) and larger (since $\pi$-conjugation increases and their $\xi$-inner product increases).

It is particularly interesting to analyze the behavior of [*n*]helicenes with *n* > 10 within the framework of the single excited state (SES) theory of ROA.[21−23] Even if, on the basis of TDDFT calculations reported in Figures SI.1−3, strict resonance is not possible with $\lambda_{exc}$ = 532 nm, from Figure 1 it is evident that the larger [*n*]helicenes are characterized by monosignated ROA spectra. This is the hallmark of SES-ROA, for which it can be shown that the ROA spectrum is simply given by the Raman spectrum multiplied by the Kuhn's dissymmetry factor $-g_{ECD}$.[21−23] The monosignated behavior of ROA can be also assessed in the lower wavenumber region of the spectra, which is reported in Figure 3. The applicability of SES-ROA can be easily checked based on the results of DFT and TDDFT calculations presented above and in the SI. In particular, for [16]helicene the $g_{ECD}$ factor for the third excited state ($S_3$), characterized by sizable dipole ($D = 41726 \times 10^{-44}$ esu$^2$ cm$^2$) and rotational ($R = -782 \times 10^{-44}$ esu$^2$ cm$^2$) strengths, is $g_{ECD} = 4R/D = -0.075$. This compares very well with the ROA/Raman intensity ratio (CID) of [16]helicene, which in the case of the D-peak at 1386 $cm^{-1}$, is 0.05. Significantly, for smaller [*n*]helicenes ROA presents both positive and negative features (see Figures 1 and 3 and the SI) indicating a condition slightly off with respect to the SES approximation; this deviation from SES behavior has indeed a counterpart in the ROA experimental data for 2-Br-hexahelicene.[18] In conclusion we can state that SES behavior takes place for longer and longer [*n*]helicenes, and this is concomitant with robustness of the D feature increasing with *n* (see Figure 2 and Figure 1).


dx.doi.org/10.1021/ct500697e | J. Chem. Theory Comput. 2014, 10, 5520−5527

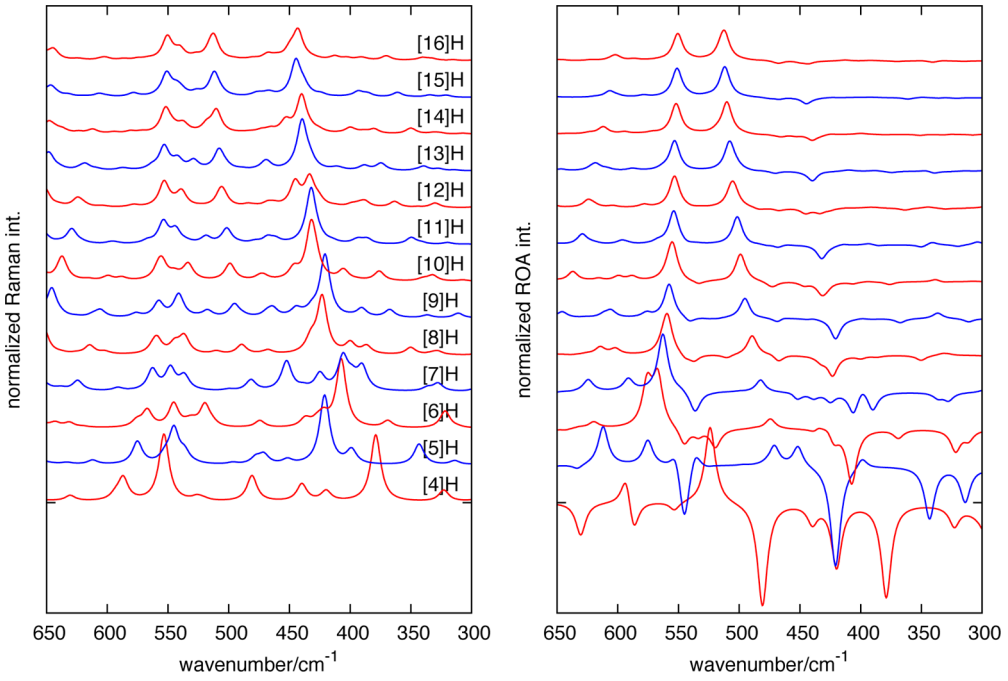


**Figure 3.** Simulated Raman (left panel) and ROA (right panel) spectra of [*n*]helicenes of increasing size (*n* = 4−16) in the low wavenumber region. Intensity and wavenumber data have been obtained from DFT calculations carried out at the B3LYP/6-31G(d,p) level. Spectra have been simulated by summing Lorentzian line shapes whose areas are proportional to the computed Raman (ROA) intensity, centered at computed vibrational frequencies. The fwhm of the Lorentzian line shapes was fixed at 10 $cm^{-1}$, and all spectra have been normalized to the strongest calculated peak.

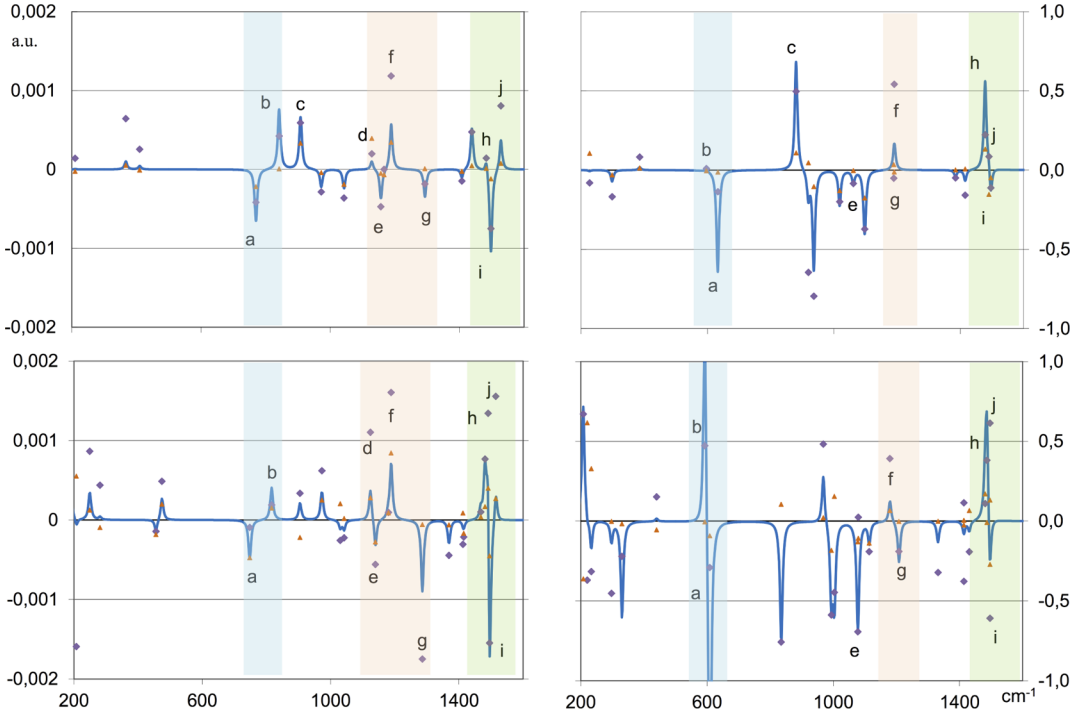


**Figure 4.** ROA calculated spectra (blue) of (1*R*)-methyloxirane (**1**) top-left panel, (1*R*,2*R*)-*trans*-dimethyl-oxirane (**2**) bottom-left panel, (1*R*)-methyl-thiirane (**3**) top-right panel, (1*R*,2*R*)-*trans*-dimethyl-thiirane (**4**) bottom-right panel. In all cases the values of the robustness parameters cos $\varphi$ and cos $\psi$ are given as blue diamonds and red triangles in correspondence of each calculated ROA band (the relative scales are on the right vertical axes). A few bands discussed in the text have been labeled, the same letter is indicative of a similarity of the corresponding normal mode (see Figure SI.6 for a pictorial view of the normal modes).

## 4. APPLICATION TO SMALL MODEL MOLECULES

As a second test case of the usefulness of the robustness parameters, we examined four molecules well-known as benchmark for ROA spectroscopy, namely (1*R*)-methyl-oxirane (**1**), (1*R*,2*R*)-*trans*-dimethyl-oxirane (**2**), (1*R*)-methyl-thiirane (**3**), and (1*R*,2*R*)-*trans*-dimethyl-thiirane (**4**). Finally a discussion on conformers of (1*S*)-epichlorohydrin (**5**) is also proposed.

In Figure SI.4 (SI, part 3) we report the ROA data of **1** that we collected in the $CCl_4$ solution: an important work comparing ROA data in the gas phase and as neat liquid is that of ref 24,


dx.doi.org/10.1021/ct500697e | J. Chem. Theory Comput. 2014, 10, 5520−5527

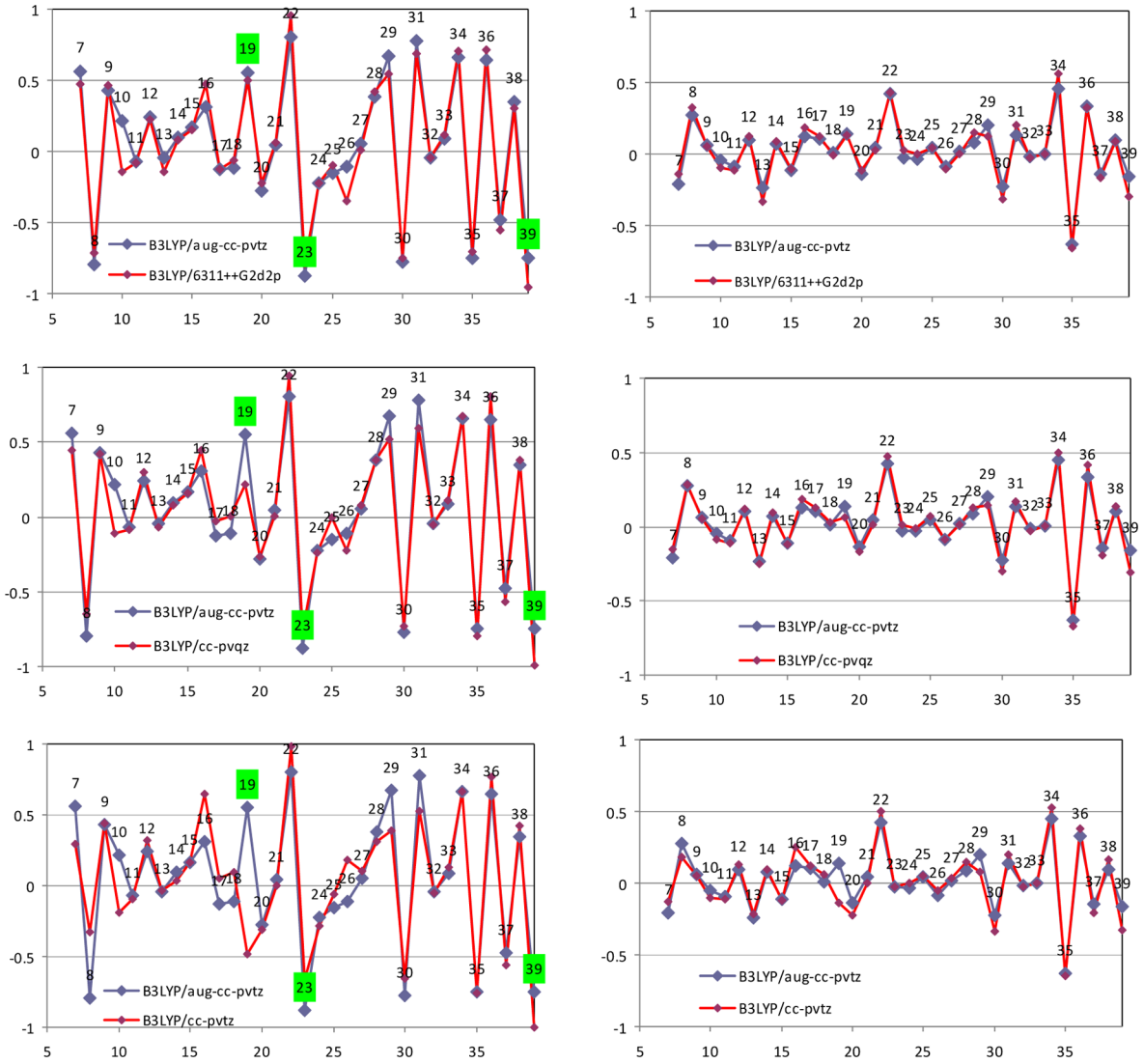


**Figure 5.** Comparison of cos $\varphi$ (left) and cos $\psi$ (right) robustness parameters for (1*R*,2*R*)-*trans*-dimethyloxirane (**2**) for various levels of calculations. Comparison is carried out by superimposing results for three different basis sets to the B3LYP/aug-cc-pvtz employed also for this and the other molecules in this work. The horizontal axis reports the sequence of normal mode numbers (low indexes correspond to low wavenumbers; indexes 1−6 refer to roto-translations, not reported).

while the first ROA data in the literature are due to ref 25. For compounds **2**−**4** we may refer to Black et al.[26] and Polavarapu et al.,[27,28] respectively. In order to show the calculated robustness, we report in Figure 4 the calculated ROA spectra of the four compounds: they compare quite well with cited literature data. In the figure the values for the robustness parameters cos $\varphi$ and cos $\psi$ are given as blue diamonds and red triangles, respectively, in correspondence of each calculated ROA band (the relative scales are on the right vertical axes); we also evidenced with letters a few bands discussed in the following. As in the case of helicenes, all values for cos $\psi$ are quite small for all bands in all molecules, while interestingly cos $\varphi$ is large (value higher than 0.5) for a few bands, especially for the two symmetric cases **2** and **4**. These same kinds of molecules were examined by Luber et al.[29] and by Cheeseman,[30] and an analogous observation was made on the $\boldsymbol{A}$ and $\boldsymbol{G}'$ contributions.

Interestingly, Cheeseman employed several functionals and basis sets and proved that all the main features are well represented with all choices:[30] indeed the most praticated application of robustness analysis in VCD has been to provide a criterion as regards the independence of calculated signs and (to a lesser extent) magnitudes of VCD features with respect to the employed level of calculation.[15]

For this reason in Figure 5 we compare the robustness parameters cos $\varphi$ (left) and cos $\psi$ (right) for the normal modes of (1*R*,2*R*)-*trans*-dimethyloxirane (**2**), by superimposing the calculated values at different levels with the results for the B3LYP/aug-cc-pvtz choice: the values of cos $\varphi$ and cos $\psi$ for normal modes next to each other in frequency are connected with a segment, for ease of understanding; a more complete version of Figure 5 is provided in Figure SI-5 of SI, part 3. Normal modes with the same number are more than 99% superimposable (in the case B3LYP/6-311++G(2d,2p) nearly degenerate normal modes 35, 36, and 37 have been reshuffled). We evidenced in green the normal modes which are robust according to cos $\varphi$, but for which one of the two values of $\xi(\boldsymbol{\alpha}, \boldsymbol{\alpha})$ and $\xi(\boldsymbol{G}', \boldsymbol{G}')$ is much smaller than the other, as shown in Table SI-2, part 3. We judge these cases not so robust. One can observe that the three methods B3LYP/aug-cc-pvtz, B3LYP/6-311++G(2d,2p), and B3PW91/aug-cc-pvtz give very similar results; only lowering


dx.doi.org/10.1021/ct500697e | J. Chem. Theory Comput. 2014, 10, 5520−5527

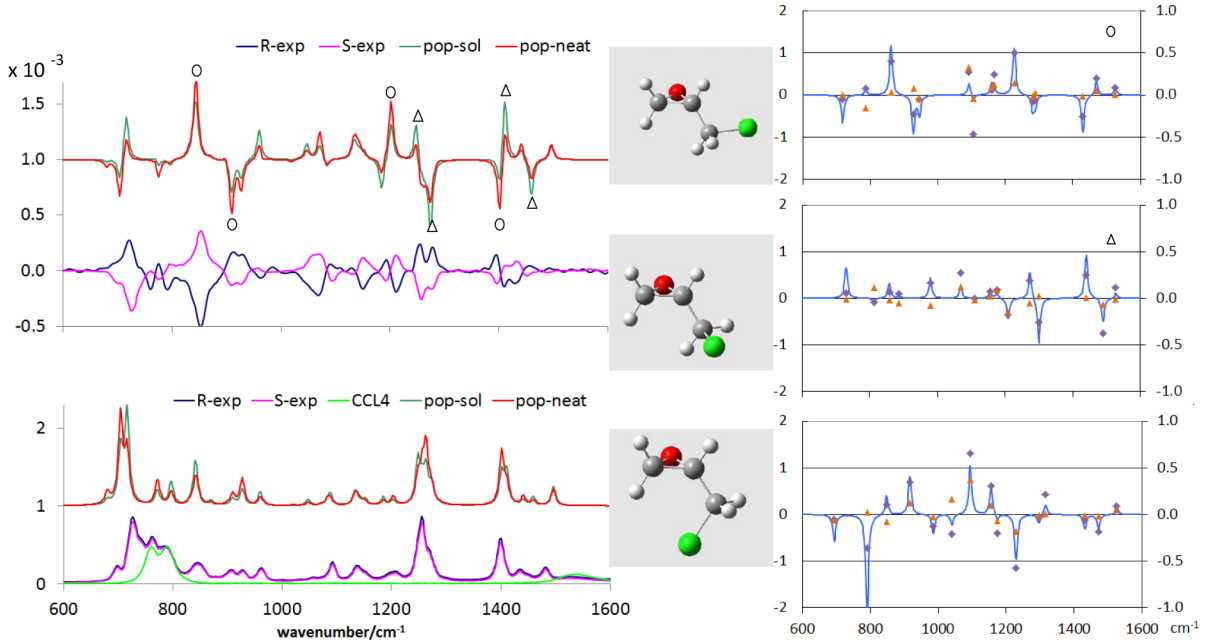


**Figure 6.** Left: Comparison of experimental ROA (top) and Raman (lower) spectra of (1*R*)- and (1*S*)-epichlorohydrin with the calculated corresponding spectra for (1*S*)-epichlorohydrin: calculated wavenumbers have been scaled by 0.98; two different conformer populations have been used attributed to $CCl_4$ solution (pop-sol) and to the neat case (pop-neat) as explained in the text. Open circles: robust bands of conformer *gauche I*; triangles: robust bands of conformer *gauche II*. Right: Calculated ROA spectra of the three conformers *gauche I*, *gauche II*, and *cis* (top down) of (1*S*)-epichlorohydrin defined in the inset. In all cases the values for the robustness parameters cos $\varphi$ and cos $\psi$ are given as blue diamonds and red triangles respectively, in correspondence of each calculated ROA band (the relative scales are on the right vertical axes). Excitation 532 nm; concentration 2.75 M.

considerably the calculation level produces problems, particularly on normal mode #19: indeed basis set 6-31G* does not adequately represent Raman and ROA data.

Robustness analysis is also useful to compare results for similar molecules. Indeed, it is quite instructive to compare the four spectra of Figure 4, considering that some features are conserved from one molecule to another, particularly between the two oxirane compounds. Obviously a large robustness parameter cannot guarantee *per se* the occurrence of a band with identical or similar characteristics in different but related molecules, since the presence of a second methyl or the substitution of an oxygen with a sulfur atom is not a small perturbation. This had been already evidenced in ref 31, considering the ring deformation modes of methyl oxirane and methyl thiirane where the frequency order of the doublet labeled **a**, **b** inverts in the two molecules. Band **b**, observed as positive in ref 31 in methyl thiirane, is not reproduced by the calculation neither in SCP (180°) geometry (as employed here) nor in ICPu/SCPu (180°) or ICPd/SCPd(90°) geometries. In any case one can recognize modes **a**, **c**, **f**, **i**, and **j** in both molecules **1** and **3**; however, the patterns of the two spectra are quite different due to shifts in frequency of the homologous modes and degeneracies (in the thiirane case) which change heavily the triplet at 1400−1500 $cm^{-1}$.

Comparison of dimethyl oxirane (**2**) and dimethyl thiirane (**4**) ROA data evidence quite different spectra (again bands due to similar modes are identified with equal letters). In the SI (part 3) we report in Tables SI.3 and SI.4 the calculated frequencies, intensities, and robustness; in Figure SI.6 we report representation of the normal modes underlying the labeled bands. The strong similarity of the methyl oxirane and dimethyl oxirane spectra, instead, is quite impressive; indeed the spectral pattern is highly conserved. The identification of similar normal modes and robustness leads us to distinguish characteristic regions with highly conserved normal modes: the region containing band **a**, corresponding to ring deformation modes; the region containing **e**, **f**, and **g**, bands, corresponding to methyl and methine deformation modes; and the region containing **i** and **j** bands, with methyl bendings.

Obviously the situation is slightly more complicated for the other molecule studied here and related to methyl oxirane, namely (1*S*)-epichlorohydrin (**5**) (see Figure 6) possessing three conformers in correspondence of the three $CH_2Cl$ group orientations, which have been called *gauche I*, *gauche II*, and *cis* (with reference to the dihedral angle formed by the C−Cl bond and the bisector of the ring, see Figure 6). As established by Wang and Polavarapu[32] by VCD, the population ratio is (*gauche I*):(*gauche II*):(*cis*) = 34.0%:58.6%:7.4% in the $CCl_4$ solution and 54.6%:35.7%:9.7% in the case of neat liquid. Also CH-stretching data in the fundamental and overtones regions[33] show contributions from *gauche I* and *gauche II* conformers, while the *cis* conformer has indeed a minor importance. Interestingly, most features of the experimental ROA spectrum appear as doublets, and, when the signs of calculated ROA spectra of *gauche I* and *gauche II* conformers are coincident, the doublets appear as split bands, while, when the signs of calculated ROA spectra of *gauche I* and *gauche II* conformers are opposite, the ROA bands appear as pseudoexcitonic couplets. Once more cos $\varphi$ is a more significant parameter for robustness than cos $\psi$. The ROA spectrum, taken in the $CCl_4$ solution at quite high concentration, appears to be better reproduced when assuming higher population of *gauche I* than *gauche II*. In Figure 6 top-left panel, the robust bands of conformer *gauche I*, labeled by open circles, are clearly observed (together with the negative nonrobust one at 720 $cm^{-1}$); robust bands of conformer *gauche II*, labeled by triangles, are less evident (the positive one at 1250 $cm^{-1}$ is not observed, the one at 1410 $cm^{-1}$ less intense than calculated). This analysis reveals how useful the robustness parameters of characteristic ROA bands may be in investigating the conformer population of flexible molecules.


dx.doi.org/10.1021/ct500697e | *J. Chem. Theory Comput.* 2014, 10, 5520−5527

ROA data suggest a slightly different situation with respect to the conclusion deduced by VCD, probably due to the high concentration of epichlorhydrin needed to carry out ROA experiments, which appears to stabilize *gauche I* conformer, as in the case of the neat liquid. More challenging cases should be considered, like, for example, L-proline, which exhibits a quite flexible five-membered ring and for which ROA spectra were taken recently.[34,35]

## 5. CONCLUSIONS

By analyzing the algebraic structure of the ROA intensity formula, we have introduced the concept of inner products among the molecular tensors involved. This allows the straightforward definition of robustness by means of the cosine of the angle formed by the tensors with respect to this definition of inner product. Two robustness parameters can be defined in this way. Cos $\varphi$ is related to the $\xi$-inner product of the electric polarizability ($\boldsymbol{\alpha}$) and the electric dipole - magnetic dipole polarizability ($\boldsymbol{G}'$) and may be called G-robustness. Cos $\psi$ is related to the Frobenius inner product of the electric polarizability ($\boldsymbol{\alpha}$) and the electric dipole - electric quadrupole tensor ($\boldsymbol{A}$) and may be called A-robustness. In the examples we have studied in this work G-robustness (cos $\varphi$) is prevalent over A-robustness (cos $\psi$), even though we cannot make a general statement on that.

The analysis ROA robustness in [$n$]helicenes of increasing size has revealed the onset of marked G-robustness (with secondary contribution from A-robustness) of D-peak collective ring-breathing vibrations, previously characterized in 2-Br-hexahelicene.[18] This is the consequence of $\pi$-conjugation effects and of the high symmetry of the system which, for large $n$ values, acquires a 6-fold helicoidal axis. Concomitantly, SES behavior has been monitored in ROA of the [$n$]helicene series.

On the other hand, small molecules with lower symmetry do not exhibit similarly large values of robustness (neither A-robustness nor G-robustness). Contrary to the case of [$n$]helicenes the ROA spectra of oxiranes and epichlorohydrin show many signals of similar relative intensity, which indicates the absence of a collective normal mode capable of conveying the large part of ROA intensity through an effective projection of the molecular polarizability onto the $\boldsymbol{G}'$ and $\boldsymbol{A}$ tensors. Under this regard we think that the theoretical usefulness of our analysis of ROA intensity is the recognition of the inner product structure, which transparently translates the molecular tensors into the observed spectroscopic quantity. Based on this result the situation for ROA becomes similar to that of VCD, where intensities are the result of the inner product of magnetic and electric transition dipole moments. On small molecules ROA robustness analysis can be helpful to conformational studies.

A larger set of molecules (in particular flexible ones) will be necessarily required to benchmark and assess the typical robustness values in ROA and determine thresholds and representative values, similarly to what has been done in VCD spectroscopy. Nevertheless, even at this early level of development, ROA robustness has proved useful to highlight collective effects in $\pi$-conjugated helical systems ([$n$]helicenes) and to distinguish persistent vibrational modes in methyl- and dimethyloxirane, and it has supported the discussion on the population of conformers of epichlorohydrin.

## ■ ASSOCIATED CONTENT

### Supporting Information

(1) Algebraic properties of $\xi$; (2) DFT data on [$n$]helicenes; (3) ROA spectroscopic data on oxirane/thiirane molecules. This material is available free of charge via the Internet at http://pubs.acs.org.

## ■ AUTHOR INFORMATION


### Corresponding Authors

*E-mail: matteo.tommasini@polimi.it.
*E-mail: giovanna.longhi@unibs.it.


### Notes

The authors declare no competing financial interest.

## ■ ACKNOWLEDGMENTS

We gratefully acknowledge J. R. Cheeseman (Gaussian, Inc.) for very helpful information on ROA tensors computed by the Gaussian09 code. M.T. thanks the Italian MIUR for financial support, under the auspices of the FIRB program RBFR08XH0H (Futuro in Ricerca 2008). B.N.O. thanks the Ministerio de Educación in Spain for the grant AP2009-2797. We acknowledge both referees for constructive advice. This work was presented at the third Italian Meeting on Raman Spectroscopy and Nonlinear Optical Effects (GISR2014, 9−11 June 2014, Parma University, Italy).

## ■ REFERENCES


(1) Barron, L. *Molecular Light Scattering and Optical Activity*; Cambridge Univ. Press: Cambridge, UK, 1982.
(2) Barron, L.; Hecht, L. In *Circular Dichroism: Priciples and Applications*; Berova, N., Nakanishi, K., Woody, R., Eds.; Wiley-VCH: New York, 2000; pp 667−702.
(3) Nafie, L. *Vibrational Optical Activity − Principles and Applications*; Wiley: New York, 2011.
(4) Hug, W. In *Comprehensive Chiroptical Spectroscopy − Vol. 1 (Instrumentation, Methodologies, and Theoretical Simulations)*; Berova, N., Polavarapu, P., Nakanishi, K., Woody, R., Eds.; John Wiley & Sons: Hoboken, NJ, USA, 2012; pp 147−178.
(5) Polavarapu, P. L. *J. Phys. Chem.* **1990**, *94*, 8106−8112.
(6) Crawford, T. *Theor. Chem. Acc.* **2006**, *115*, 227−245.
(7) Pecul, M.; Ruud, K. *Int. J. Quantum Chem.* **2005**, *104*, 816−829.
(8) Pecul, M.; Lamparska, E.; Cappelli, C.; Frediani, L.; Ruud, K. *J. Phys. Chem. A* **2006**, *110*, 2807−2815.
(9) Liégeois, V.; Ruud, K.; Champagne, B. *J. Chem. Phys.* **2007**, *127*, 204105.
(10) Crawford, T. D.; Ruud, K. *ChemPhysChem* **2011**, *12*, 3442−3448.
(11) Weymuth, T.; Haag, M. P.; Kiewisch, K.; Luber, S.; Schenk, S.; Jacob, C. R.; Herrmann, C.; Neugebauer, J.; Reiher, M. *J. Comput. Chem.* **2012**, *33*, 2186−2198.
(12) Autschbach, J. *Chirality* **2009**, *21*, E116−E152.
(13) Barron, L.; Buckingham, A. *Mol. Phys.* **1971**, *20*, 1111−1119.
(14) Barron, L. D.; Buckingham, A. D. *Chem. Phys. Lett.* **2010**, *492*, 199−213.
(15) Nicu, V. P.; Baerends, E. J. *Phys. Chem. Chem. Phys.* **2009**, *11*, 6107−6118.
(16) Gobi, S.; Magyarfalvi, G. *Phys. Chem. Chem. Phys.* **2011**, *13*, 16130−16133.
(17) Covington, C. L.; Polavarapu, P. L. *J. Phys. Chem. A* **2013**, *117*, 3377−3386.
(18) Johannessen, C.; Blanch, E. W.; Villani, C.; Abbate, S.; Longhi, G.; Agarwal, N. R.; Tommasini, M.; Lightner, D. A. *J. Phys. Chem. B* **2013**, *117*, 2221−2230.
(19) Castiglioni, C.; Tommasini, M.; Zerbi, G. *Philos. Trans. R. Soc., A* **2004**, *362*, 2425−2459.
(20) Frisch, M. J.; Trucks, G. W.; Schlegel, H. B.; Scuseria, G. E.; Robb, M. A.; Cheeseman, J. R.; Scalmani, G.; Barone, V.; Mennucci, B.; Petersson, G. A.; Nakatsuji, H.; Caricato, M.; Li, X.; Hratchian, H. P.; Izmaylov, A. F.; Bloino, J.; Zheng, G.; Sonnenberg, J. L.; Hada, M.; Ehara, M.; Toyota, K.; Fukuda, R.; Hasegawa, J.; Ishida, M.; Nakajima, T.; Honda, Y.; Kitao, O.; Nakai, H.; Vreven, T.; Montgomery, J. A., Jr.;

Peralta, J. E.; Ogliaro, F.; Bearpark, M.; Heyd, J. J.; Brothers, E.; Kudin, K. N.; Staroverov, V. N.; Kobayashi, R.; Normand, J.; Raghavachari, K.; Rendell, A.; Burant, J. C.; Iyengar, S. S.; Tomasi, J.; Cossi, M.; Rega, N.; Millam, J. M.; Klene, M.; Knox, J. E.; Cross, J. B.; Bakken, V.; Adamo, C.; Jaramillo, J.; Gomperts, R.; Stratmann, R. E.; Yazyev, O.; Austin, A. J.; Cammi, R.; Pomelli, C.; Ochterski, J. W.; Martin, R. L.; Morokuma, K.; Zakrzewski, V. G.; Voth, G. A.; Salvador, P.; Dannenberg, J. J.; Dapprich, S.; Daniels, A. D.; Farkas, O.; Foresman, J. B.; Ortiz, J. V.; Cioslowski, J.; Fox, D. J. *Gaussian 09 Revision D.01*; Gaussian Inc.: Wallingford, CT, 2009.

(21) Nafie, L. A. *Chem. Phys.* **1996**, *205*, 309−322.

(22) Vargek, M.; Freedman, T.; Lee, E.; Nafie, L. *Chem. Phys. Lett.* **1998**, *287*, 359−364.

(23) Nafie, L. A. *Theor. Chem. Acc.* **2008**, *119*, 39−55.

(24) Sebestik, J.; Bour, P. *J. Phys. Chem. Lett.* **2011**, *2*, 498−502.

(25) Bose, P.; Polavarapu, P.; Barron, L.; Hecht, L. *J. Phys. Chem.* **1990**, *94*, 1734−1740.

(26) Black, T. M.; Bose, P. K.; Polavarapu, P. L.; Barron, L. D.; Hecht, L. *J. Am. Chem. Soc.* **1990**, *112*, 1479−1489.

(27) Bose, P.; Barron, L.; Polavarapu, P. *Chem. Phys. Lett.* **1989**, *155*, 423−429.

(28) Polavarapu, P.; Pickard, S.; Smith, H.; Black, T.; Barron, L.; Hecht, L. *Talanta* **1993**, *40*, 545−549.

(29) Luber, S.; Herrmann, C.; Reiher, M. *J. Phys. Chem. B* **2008**, *112*, 2218−2232.

(30) Cheeseman, J. R.; Frisch, M. J. *J. Chem. Theory Comput.* **2011**, *7*, 3323−3334.

(31) Barron, L.; Polavarapu, P. *Mol. Phys.* **1988**, *65*, 659−667.

(32) Wang, F.; Polavarapu, P. L. *J. Phys. Chem. A* **2000**, *104*, 6189−6196.

(33) Abbate, S.; Longhi, G.; Castiglioni, E. In *Comprehensive Chiroptical Spectroscopy − Vol. 1 (Instrumentation, Methodologies, and Theoretical Simulations)*; Berova, N., Polavarapu, P., Nakanishi, K., Woody, R., Eds.; John Wiley & Sons: Hoboken, NJ, USA, 2012; pp 247−273.

(34) Kapitán, J.; Baumruk, V.; Bour, P. *J. Am. Chem. Soc.* **2006**, *128*, 2438−2443.

(35) Qiu, S.; Li, G.; Wang, P.; Zhou, J.; Feng, Z.; Li, C. *J. Phys. Chem. A* **2011**, *115*, 1340−1349 PMID: 21309515.